

# Single-photon scattering and bound states in a one-dimensional waveguide with giant atom

Wei Zhao<sup>1</sup> and Zhihai Wang<sup>1,\*</sup>

<sup>1</sup>Center for Quantum Sciences and School of Physics,  
Northeast Normal University, Changchun 130024, China

In this paper, we investigate the single-photon scattering and bound states in a one-dimensional coupled resonator waveguide which couples to a single giant atom. When the atom couples to the waveguide via two resonators, the single-photon reflection rate is characterized by either Breit-Wigner or Fano line shapes, depending on the spatial size of the atom. When the atom couples to the waveguide via multiple resonators, we numerically show that the single-photon complete reflection results from the destructive interference effect. We also find a phase transition phenomena for the multi-resonator coupling case, which reveals that the upper bound state only exists when the atom-waveguide coupling strength is above a critical value.

## I. INTRODUCTION

The light-matter interaction is a central topic in the field of quantum optics. Recent years, much attention has been focused on the light-matter interaction in waveguiding structures, leading to a scenario named as waveguide QED. As reviewed in Refs. [1, 2] and the references therein, there are lots of theoretical and experimental works on waveguide QED system, for example, the single-photon device [3–5], the phase transition [6, 7], dressed or bound states [8–13], the exotic topological and chiral phenomena [14–19], just name a few.

In the sense of quantum network [20], the waveguide is usually regarded as quantum channel for photons, and the atom (or artificial atom) plays as quantum node. One of the subject in waveguide QED is how to control the propagation of the photons in quantum channel by adjusting the quantum node(s). In the traditional scheme, the size of the atom is at least one order smaller than the wavelength of the propagating photons in the waveguide, therefore it is reasonable to approximate the atom as a point-like dipole. Recently, a superconducting transmon qubit was successfully coupled to propagating surface acoustic waves [21–24]. Due to the slow propagation speed of sound in solids, the wavelength of the phonons for a given frequency can be smaller than the size of the atom, and the point-like dipole approximation for the atom does not work. In this situation, we must deal with a “giant atom” (GA) setup [25–34], in which the size of the atom provides us another controller besides the resonant frequency and the dipole moment, for the states of the photons in the waveguide.

In this paper, we investigate the single-photon scattering and bound states in a one-dimensional coupled-resonator waveguide with GA, which can be coupled to the waveguide via two or multiple resonators. For the two-resonator coupling situation, we analytically obtain the single-photon scattering behavior and find that

the Breit-Wigner or Fano [35] line shapes for the reflection rate take turns as the size of the GA changes. For multiple-resonator coupling situation, we numerically demonstrate the destructive interference, which finally leads to the complete single-photon reflection. Besides, we find a phase transition phenomena when the GA couples to the waveguide via multiple resonators. That is, when the atom-waveguide coupling strength surpasses a certain value, there will be two bound states asymmetrically located above and below the propagating band, otherwise, there will be only one, which locates below the propagating band.

The rest of the paper is organized as follows. In Sec. II, we present our model and the Hamiltonian. In Sec. III and IV, we study the single-photon scattering when the GA couples to the waveguide via two and multiple resonators, respectively. In Sec. V, we discuss the properties of the bound states and end up with a brief conclusion in Sec. VI. Some detailed derivation in the momentum space is given in the Appendix.

## II. MODEL AND HAMILTONIAN

As schematically shown in Fig. 1(a), the system we consider is composed by a one-dimensional coupled-resonator waveguide with infinite length and a two-level system. Such system can be realized in the superconducting quantum circuits which is demonstrated in Fig. 1(b). Here, the LC circuits (LCC) serve as the resonators, and the transmon qubit serves as the two-level system. The capacities couple the resonators as well as the resonators and the transmon. In the conventional photonic waveguide scenario, the natural atom (for example, the Rydberg atom) only coupled to a single resonator due to its small size. However, we now study the effect of a GA scheme, where the two-level system can be coupled to the waveguide via two or more resonators simultaneously.

The coupled-resonator waveguide is modelled by the Hamiltonian

$$H_c = \omega \sum_j a_j^\dagger a_j - \xi \sum_j \left( a_{j+1}^\dagger a_j + a_j^\dagger a_{j+1} \right), \quad (1)$$

\* wangzh761@nenu.edu.cn

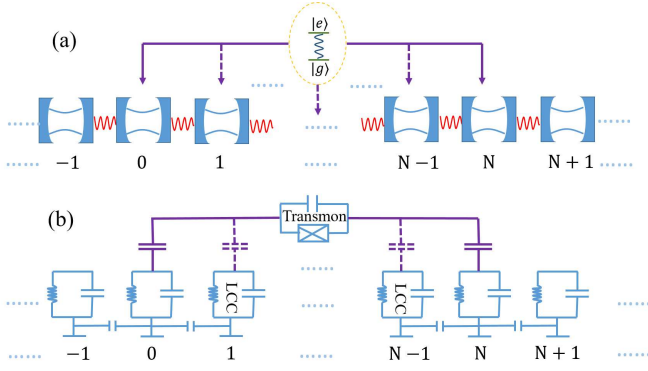


FIG. 1. (a) Schematic configuration for a one-dimensional coupled-resonator waveguide coupled to a giant atom. The solid purple solid lines represent that the giant atom couples to two resonators. The purple solid together with the dashed lines represent that the giant atom couples to multiple resonators. (b) The effective circuit diagram of the device. The solid and dashed purple lines represent the same meaning with (a).

where  $\omega_c$  is frequency of the resonators, and  $a_j$  is the bosonic annihilation operator on site  $j$ .  $\xi$  is the hopping strength between the nearest resonators.

We now formulate the interaction between the GA and the waveguide. In this paper, we will discuss the single-photon scattering and bound states in two kinds of setups as follows. In case (I), the GA only couples to the 0th and the  $N$ th resonators with the same coupling strength  $J$ , the Hamiltonian for the whole system is written as

$$H_1 = H_c + \Omega|e\rangle\langle e| + J[(a_0^\dagger + a_N^\dagger)\sigma^- + \text{H.c.}] \quad (2)$$

where  $\sigma^\pm$  are the usual Pauli operators of the GA, and  $\Omega$  is the transition frequency between the ground state  $|g\rangle$  and the excited state  $|e\rangle$ . In case (II), the GA uniformly couples to  $N+1$  resonators with the resonator number  $j = 0 \rightarrow N$  simultaneously. The Hamiltonian is expressed as

$$H_2 = H_c + \Omega|e\rangle\langle e| + \frac{2J}{N+1} \sum_{i=0}^N (a_i^\dagger \sigma^- + \text{H.c.}) \quad (3)$$

We note that, the total coupling strength between the GA and the waveguide are both  $2J$  for the two cases. Here, we have performed the rotating wave approximation, which is valid in the parameter regime  $J \ll \Omega$  and  $\Omega \sim \omega_c$ .

The model can be realized in a superconducting quantum circuits scheme as shown in Fig. 1(b), where a superconducting qubit named as transmon [36] couples to the waveguide composed by coupled LC resonators. The hopping interaction will be present between any two resonators, but the strength decreases fast with their distance. Therefore, we only consider the nearest inter-resonator coupling and perform the rotating wave approximation in the situation of  $\xi \ll \omega_c$ . The waveguide

supplies a propagating channel for the photons and it forms an energy band, which is centered at  $\omega_c$  and the total width is  $4\xi$ .

### III. SINGLE-PHOTON SCATTERING WITH TWO COUPLING RESONATORS

In this section, we will study the single-photon scattering in case (I), that is, the GA only couples to the 0th and  $N$ th resonators in the waveguide. We now consider that a single photon with wave vector  $k$  is incident from the left side of the waveguide. Since the excitation number in the system conserves, the eigenstate in the single-excitation subspace can be written as

$$|E_k\rangle = \left( \sum_j c_j a_j^\dagger + u_e \sigma^+ \right) |G\rangle, \quad (4)$$

where  $|G\rangle$  represents that all of the resonators in the waveguide are in the vacuum states, while the GA is in the ground state  $|g\rangle$ .  $c_j$  is the probability amplitude for finding a photonic excitation in resonator  $j$ , and  $u_e$  is the excitation amplitude of the GA. In the regime  $j < 0$  and  $j > N$ , the amplitude  $c_j$  can be written in the form of

$$c_j = \begin{cases} e^{ikj} + r e^{-ikj} & j < 0 \\ t e^{ikj} & j > N \end{cases}, \quad (5)$$

where  $r$  and  $t$  are respectively the single-photon reflection and transmission amplitudes. Hereafter, the wave vector  $k$  is considered to be dimensionless by setting the distance between two arbitrary neighboring resonators as unit. In the regime covered by the GA, the photon propagates back and forth, and the amplitude  $c_j$  for  $0 \leq j \leq N$  can be expressed as

$$c_j = A e^{ikj} + B e^{-ikj}. \quad (6)$$

The Schödinger equation  $H_1|E_k\rangle = E_k|E_k\rangle$  yields the dispersion relation  $E_k = \omega_c - 2\xi \cos k$ . Together with the continuous condition at  $j = 0$  and  $j = N$ , which are  $1 + r = A + B$  and  $A e^{ikN} + B e^{-ikN} = t e^{ikN}$ , respectively, the reflection rate  $R = |r|^2$  can be obtained as

$$R = \frac{4J^4 \cos^4\left(\frac{kN}{2}\right)}{4J^4 \cos^4\left(\frac{kN}{2}\right) + [\xi \Delta_k \sin k - J^2 \sin(kN)]^2}, \quad (7)$$

where  $\Delta_k = E_k - \Omega$  is the detuning between the GA and the propagating photons in the waveguide.

In the small atom scenario ( $N = 0$ ), we recover the results given in Ref. [5], and it is obvious that the incident photon will be completely reflected ( $R = 1$ ) when it is resonant with the atom, that is,  $\Delta_k = 0$ . However, for the GA situation under our consideration, the photon can be reflected by the two connecting points, the scattering process will be dramatically affected by the size of the GA. In Fig. 2, we plot the reflection rate  $R$  as a function

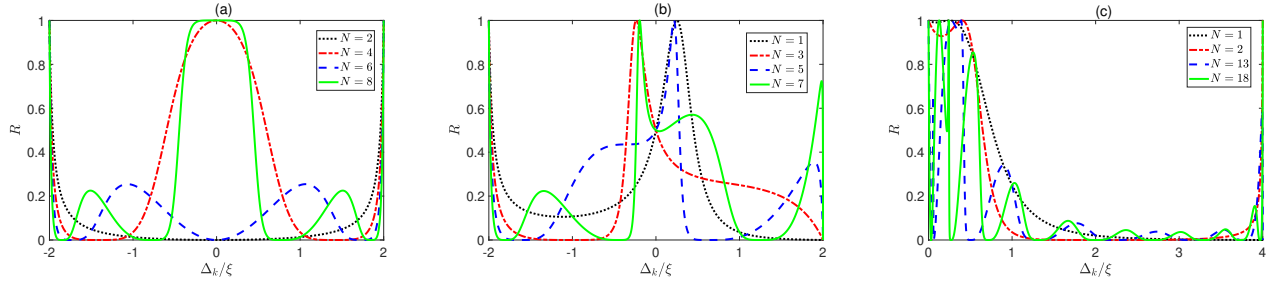


FIG. 2. The reflection rate  $R$  as a function of the detuning  $\Delta_k$  for different  $N$  with two coupling resonators. The parameters are set as  $J = 0.5\xi$ ,  $\omega_c = 20\xi$ .  $\Omega = 20\xi$  for (a) and (b), and  $\Omega = 18\xi$  for (c).

of the detuning for different  $N$ , which characterizes the size of the GA.

Let us first discuss the situation of  $\omega_c = \Omega$ . In this case, the GA is resonant to the propagating photons with wave vector  $k = \pi/2$ . In Fig. 2(a) and (b), we demonstrate the results for even and odd  $N$ , respectively. For even  $N$  in Fig. 2(a), the incident photon will be completely transmitted ( $R = 0$ ) for  $N = 4m + 2$  and completely reflected ( $R = 1$ ) for  $N = 4m$  ( $m = 0, 1, 2, \dots$ ). Furthermore, the curve always represents a Breit-Wigner-like line shape around the resonance  $\Delta_k = 0$ , which is similar to the small atom case. Meanwhile, for odd  $N$ , we observe a frequency shift in Fig. 2(b), with the complete reflection occurring at a positive (negative) detuning for  $N = 4m + 1$  ( $4m + 3$ ), and the curve behaves as a Fano-like shape around the peak, which is not for small atom situation. Moreover, we can also find that  $R = 0.5$  for  $\Delta_k = 0$ , which is independent of the size of GA.

Next, we consider the situation of  $\omega_c \neq \Omega$ . As shown in Fig. 2(c), the reflection rate shows a complicated dependence on the detuning  $\Delta_k$ . From Eq. (7), the detuning for complete reflection is determined by the transcendental equation

$$\Delta_k = \frac{J^2 \sin(kN)}{\xi \sin k}, \quad (8)$$

around which, the reflection yields a Fano shape. We also observe that, there will be one or more complete reflection frequencies (excluding the edge of the photonic propagating bands), depending on the values of  $N$ . It implies that, we can design the on-demand single-photon transistor by adjusting the size of GA in our waveguide setup.

#### IV. SINGLE-PHOTON SCATTERING WITH MULTIPLE COUPLING RESONATORS

Now, we move to case (II), where the GA couples to all of the resonators it covers, and the Hamiltonian of the system is described by Eq. (3). In this case, we will give a semi-analytical result for the single-photon scattering behavior.

We note that the Hamiltonian in Eq. (3) can be rewritten as  $H_2 = H_L + H_R + H_s + H_{\text{Int}}$ , where

$$H_L = \sum_{j=-\infty}^{-1} \omega_c a_j^\dagger a_j - \xi \sum_{j=-\infty}^{-2} (a_j^\dagger a_{j+1} + a_{j+1}^\dagger a_j), \quad (9)$$

$$H_R = \sum_{j=N+1}^{\infty} \omega_c a_j^\dagger a_j - \xi \sum_{j=N+1}^{\infty} (a_j^\dagger a_{j+1} + a_{j+1}^\dagger a_j), \quad (10)$$

$$H_s = \Omega |e\rangle \langle e| + \omega_c \sum_{j=0}^N a_j^\dagger a_j + \frac{2J}{N+1} \sum_{j=0}^N (a_j^\dagger \sigma^- + \text{H.c.}) \\ = \sum_m v_m |\phi_m\rangle \langle \phi_m| \quad (11)$$

$$H_{\text{Int}} = -\xi \sum_m (a_{-1}^\dagger x_m |0\rangle \langle \phi_m| + a_{N+1}^\dagger y_m |0\rangle \langle \phi_m| + \text{H.c.}), \quad (12)$$

Here,  $v_m$  ( $m = 1, 2, \dots, N+2$ ) is the  $m$ th eigen value of  $H_s$  in the single-excitation subspace and  $|\phi_m\rangle$  is the corresponding eigen state, and  $x_m = \langle 0|a_0|\phi_m\rangle$ ,  $y_m = \langle 0|a_N|\phi_m\rangle$ . As before, we assume that a single photon with wave vector  $k$  is incident from the left side of the waveguide, the wave function in the single-excitation subspace follows

$$|\psi_k\rangle = \sum_{j=-\infty}^{-1} U_j a_j^\dagger |0\rangle + \sum_{j=N+1}^{\infty} V_j a_j^\dagger |0\rangle + \sum_m A_m |\phi_m\rangle, \quad (13)$$

where  $U_j = e^{ikj} + r e^{-ikj}$ ,  $V_j = t e^{ikj}$ , with  $r$  and  $t$  being the reflection and transmission amplitudes. The eigen function  $H_2 |\psi_k\rangle = E_k |\psi_k\rangle$  yields  $E_k = \omega_c - 2\xi \cos k$  and

$$(E_k - \omega_c) U_{-1} = -\xi \sum_m x_m A_m - \xi U_{-2}, \quad (14)$$

$$(E_k - \omega_c) V_{N+1} = -\xi \sum_m y_m A_m - \xi V_{N+2}, \quad (15)$$

$$(E_k - v_m) A_m = -\xi (U_{-1} x_m^* + V_{N+1} y_m^*). \quad (16)$$

Even without the detailed calculation about the scattering behavior, we can obtain the condition for a complete reflection ( $t = 0$ ) from Eq. (15), which yields

$$\sum_m y_m A_m = 0. \quad (17)$$

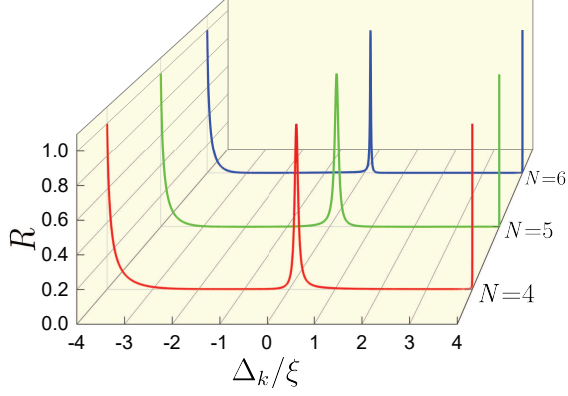


FIG. 3. The reflection rate  $R$  as a function of the detuning  $\Delta_k$  for different  $N$  with multiple coupling resonators. The parameters are set as  $J = 0.5\xi$ ,  $\omega_c = \Omega = 20\xi$ .

It implies that the incident photon will interact with all of the modes of  $H_s$ , and the destructive interference will lead to a complete reflection. The similar mechanism was also found in a super-cavity scheme under the two-mode approximation [37].

Furthermore, the single-photon scattering behavior can be predicted by solving Eqs. (14), (15) and (16), and the reflection rate  $R = |r|^2$  is obtained as

$$R = \frac{(Q_1 Q_2 + \xi^2 \sin^2 k - |M_3|^2)^2 + \xi^2 (Q_1 - Q_2)^2 \sin^2 k}{(Q_1 Q_2 - \xi^2 \sin^2 k - |M_3|^2)^2 + \xi^2 (Q_1 + Q_2)^2 \sin^2 k}, \quad (18)$$

where  $Q_n = E_k - \omega_c - M_n + \xi \cos k$  for  $n = 1, 2$  and

$$M_1 = \xi^2 \sum_m \frac{|x_m|^2}{E_k - v_m}, \quad (19)$$

$$M_2 = \xi^2 \sum_m \frac{|y_m|^2}{E_k - v_m}, \quad (20)$$

$$M_3 = \xi^2 \sum_m \frac{x_m y_m^*}{E_k - v_m}, \quad (21)$$

and the condition for complete reflection is given by  $|M_3| = 0$ . In Fig. 3, we plot  $R$  as a function of  $\Delta_k$  for different relative small  $N$  and it shows that the complete reflection occurs near the resonant point  $\Delta_k = 0$ .

## V. BOUND STATES

In the above sections, we have investigated the scattering states in the single-excitation subspace, with the eigen-energy inside the band  $\omega_k \in [\omega_c - 2\xi, \omega_c + 2\xi]$ . Besides, the interaction between the GA and the waveguide breaks the translational symmetry of the waveguide, leading to another kind of bound state, where the photonic excitation is bounded near the regime of the GA,

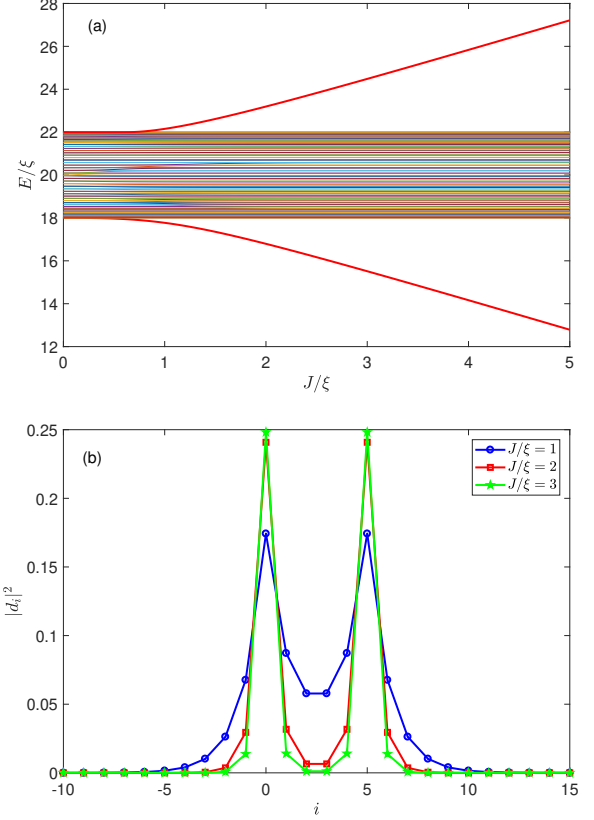


FIG. 4. The energy spectrum (a) and the photonic wave function of the bound state (b) reflection rate in Case (I). The parameters are set as  $\omega = \Omega = 20\xi$ ,  $N = 5$ .

and the corresponding energies lay outside the propagating band.

In principal, the energies for the bound state(s) can be obtained by transforming to the momentum space and solving the transcendental equation. Similar to the approach given in Ref. [9], and after the detailed calculations as shown in the Appendix, the transcendental equations for the energy  $E$  are

$$E - \Omega = \frac{J^2}{\pi} \int_{-\pi}^{\pi} dk \frac{1 + \cos(kN)}{E - \omega + 2\xi \cos(k)} \quad (22)$$

and

$$E - \Omega = \frac{2J^2}{(N+1)^2\pi} \int_{-\pi}^{\pi} dk \frac{\sin^2[\frac{k(N+1)}{2}]}{\sin^2(\frac{k}{2})[E - \omega + 2\xi \cos(k)]} \quad (23)$$

for Case (I) and Case (II), respectively. However, the integrals in the above two equations are not easy to be performed. Therefore, we will resort to numerical diagonalization of the Hamiltonian in the real space, and plot the single-excitation energy spectrum and the photonic distribution of the upper and lower states [the wave-function is expressed as  $|E\rangle = (\sum_i d_i a_i^\dagger + d_e \sigma^+) |G\rangle$ ] in Fig. 4 and Fig. 5 under the periodical boundary condition.

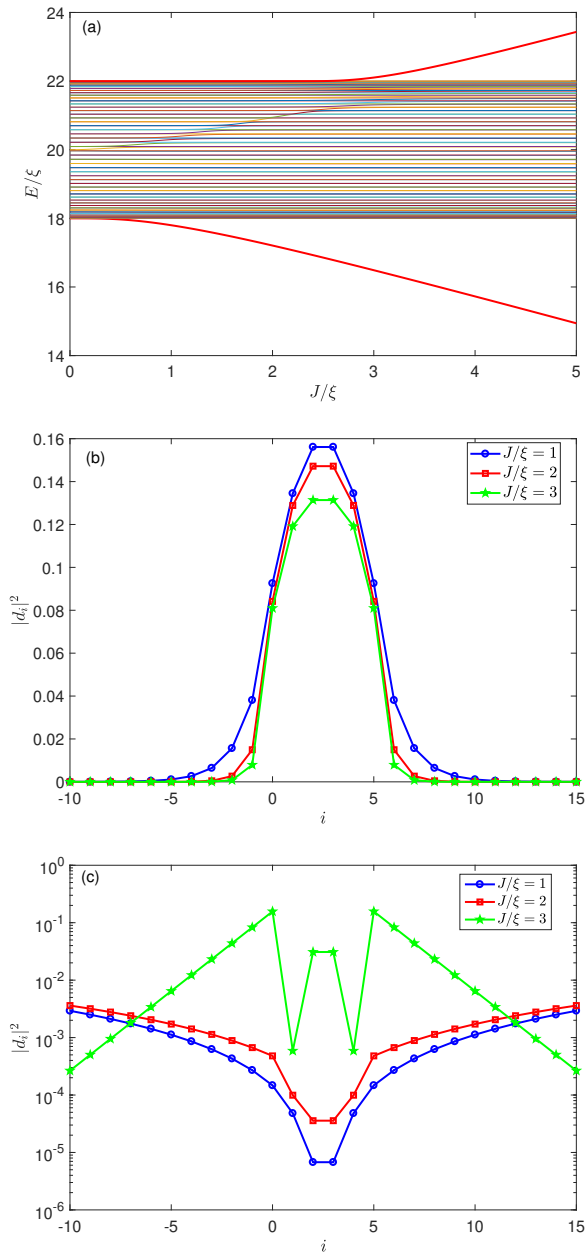


FIG. 5. The energy spectrum (a) and the photonic wave function of the lower state (b) and upper state (c) in energy for Case (II). The parameters are same with Fig. 4.

In Fig. 4(a), we plot the energy spectrum in the single-excitation subspace for Case (I), where the GA couples to the waveguide via two resonators. The energy band in the middle with band width  $4\xi$  is the scattering states, which are discussed in Sec. III. The other two red curves, which are nearly symmetrically located above and below the propagating band are the bound states. The photonic wave functions for these two states are nearly same, and are plotted in Fig. 4 (b). It shows that the photon is bounded around the two resonators which couple to the GA, and exponentially decays in the regime far from the

GA.

As for Case (II), where the GA couples to all of the resonators it covers, the upper and lower energy levels are not symmetric about the propagating band as shown in Fig. 5(a). For an arbitrary non-zero atom-waveguide  $J$ , the lower energy level is always separated from the band, and the photon is bounded in the whole regime of the GA as shown in Fig. 5(b). However, the property of the upper state depends on the value of  $J$ . For small  $J$ , the upper energy level coincides with the edge of the propagating band, as shown in Fig. 5(a). The corresponding photonic wave function is shown in Fig. 5(c). It shows that the amplitude for finding a photon in the resonator increases as it moves far away from the GA for  $J/\xi = 1$  and  $J/\xi = 2$ . It implies that the bound state with energy higher than the propagating band does not exist for small  $J$ . Only for a larger  $J$ , this energy level will be separated, and the state becomes a bound one. However, the photon distribution is still different from the lower one in that the photon mainly distributes at the two ends of the GA, and decays outside the GA regime as shown by the curve for  $J/\xi = 3$  in Fig. 5(c). We note that the similar “quantum phase transition” behavior associated with the upper bound state also exists in the waveguide setup, which couples to a small three-level atom [7].

## VI. CONCLUSION

In this paper, we have studied the single-photon scattering and bound states in a one-dimensional coupled-resonator waveguide with a dressed giant atom. The giant atom can couple to the waveguide via two or multiple resonators, and the back and forth propagation of the photons in the regime of GA will lead to some exotic phenomena. For the case of two-resonator coupling, the curve of the reflection rate will behave as either Breit-Wigner or Fano line shape, depending on the size of the GA, and the energies for the bound state lie symmetrically around the propagating band for arbitrary atom-waveguide coupling strength. For the case of multi-resonator coupling, we numerically demonstrate the destructive interference effect which leads to the single-photon complete reflection. Moreover, we find the phase transition phenomenon based on the bound states. That is, the upper bound state in which the photon locates at the end of the giant atom only exists when the atom-waveguide coupling strength surpasses a critical value.

We hope that our study will be applicable to quantum acoustics [38, 39], where the size of the emitter can be comparable to the wavelength of the phonons, and serves as a controller to the propagation of the phonons.

## ACKNOWLEDGMENTS

We thank J. L. Li for his help on figure polishing. This work is supported by National Natural Science



Foundation of China (Grant No. 11875011); Educational Commission of Jilin Province of China (Grant No. JJKH20190266KJ).

### Appendix A: Sing-photon bound states

In Eqs. (22) and (23), we have listed the transcendental equations for the energy of the bound states, when the GA couples to the waveguide via two and multiple resonators, respectively. Here, we will give the detailed derivation by transforming to the momentum space.

First, for the case in which the GA couples to the waveguide via two resonators, the Hamiltonian in the momentum space is expressed as

$$H_1 = \sum_k \omega_k a_k^\dagger a_k + \Omega |e\rangle \langle e| + \frac{J}{\sqrt{N_0}} \sum_k [a_k^\dagger (1 + e^{ikN}) \sigma^- + \text{H.c.}], \quad (\text{A1})$$

where  $a_k = \sum_{n=-\infty}^{\infty} \exp(-ikn) a_n / \sqrt{N_0}$ , with  $N_0$  the length of the waveguide, and the dispersion relation is given by  $\omega_k = \omega_c - 2\xi \cos k$ . In the single-excitation subspace, the wave function has the form

$$|\psi\rangle = (b\sigma^+ + \sum_k c_k a_k^\dagger) |G\rangle, \quad (\text{A2})$$

then the Schrodinger equation  $H_1|\psi\rangle = E|\psi\rangle$  will give the coupled equations

$$b(E - \Omega) = \frac{J}{\sqrt{N_0}} c_k (1 + e^{-ikN}), \quad (\text{A3})$$

$$(E - \omega + 2\xi \cos k) c_k = \frac{J}{\sqrt{N_0}} (1 + e^{ikN}) b. \quad (\text{A4})$$

As a result, eliminating  $c_k$ , we will obtain

$$E - \Omega = \frac{J^2}{N_0} \sum_k \frac{2[1 + \cos(kN)]}{E - \omega + 2\xi \cos(k)} = \frac{J^2}{\pi} \int_{-\pi}^{\pi} \frac{1 + \cos(kN)}{E - \omega + 2\xi \cos(k)}, \quad (\text{A5})$$

which is Eq. (22) in the main text.

Second, we consider the case that the GA couples to all of the resonators it covers in the waveguide, the Hamiltonian in the momentum space becomes

$$H_2 = \sum_k \omega_k a_k^\dagger a_k + \Omega |e\rangle \langle e| + \frac{2J}{\sqrt{N_0}(N+1)} \sum_{n=0}^N \sum_k [a_k^\dagger e^{ikn} \sigma^- + \text{H.c.}]. \quad (\text{A6})$$

Reduplicating the process from Eq. (A2) to (A5), we will end with

$$E - \Omega = \frac{2J^2}{(N+1)^2\pi} \int_{-\pi}^{\pi} dk \frac{\sin^2[\frac{k(N+1)}{2}]}{\sin^2(\frac{k}{2})[E - \omega + 2\xi \cos(k)]}, \quad (\text{A7})$$

which is Eq. (23) in the main text.

- 
- [1] D. Roy, C. M. Wilson, and O. Firstenberg, *Rev. Mod. Phys.* **89**, 021001 (2017).
  - [2] X. Gu, A. F. Kockum, A. Miranowicz, Y.-X. Liu, and F. Nori, *Phys. Rep.* **718**, 1 (2017).
  - [3] J. T. Shen and S. Fan, *Phys. Rev. Lett.* **95**, 213001 (2005).
  - [4] D. E. Chang, A. S. Sørensen, E. A. Demler, and M. D. Lukin, *Nature Phys.* **3**, 807 (2007).
  - [5] L. Zhou, Z. R. Gong, Y. X. Liu, C. P. Sun, and F. Nori, *Phys. Rev. Lett.* **101**, 100501 (2008).
  - [6] M. Fitzpatrick, N. M. Sundaresan, A. C. Y. Li, J. Koch, and A. A. Houck, *Phys. Rev. X* **7**, 011016 (2017).
  - [7] L. Qiao, Y.-J. Song, and C.-P. Sun, *Phys. Rev. A* **100**, 013825 (2019).
  - [8] H. Zheng, D. J. Gauthier, and H. U. Baranger, *Phys. Rev. A* **82**, 063816 (2010).
  - [9] G. Calajó, F. Ciccarello, D. Chang, and P. Rabl, *Phys. Rev. A* **93**, 033833 (2016).
  - [10] T. Shi, Y.-H. Wu, A. González-Tudela, and J. I. Cirac, *Phys. Rev. X* **6**, 021027 (2016).
  - [11] E. Sánchez-Burillo, D. Zueco, L. Martín-Moreno, and J. J. G.-Ripoll, *Phys. Rev. A* **96**, 023831 (2017).
  - [12] P. T. Fong and C. K. Law, *Phys. Rev. A* **96**, 023842 (2017).
  - [13] G. Calajó, Y.-L. L. Fang, H. U. Baranger, and F. Ciccarello, *Phys. Rev. Lett.* **122**, 073601 (2019).
  - [14] M. Ringel, M. Pletyukhov, and V. Gritsev, *New J. Phys.* **16**, 113030 (2014).
  - [15] V. Yannopapas, *Int. J. Mod. Phys. B* **28**, 1441006 (2014).
  - [16] I. M. Mirza and J. C. Schotland, *Phys. Rev. A* **94**, 012302 (2016).
  - [17] C. G.-Ballester, E. Moreno, F. J. Garcia-Vidal, and A. G.-Tudela, *Phys. Rev. A* **94**, 063817 (2016).
  - [18] M. Bello, G. Platero, J. I. Cirac, and A. G.-Tudela, *Sci. Adv.* **5**, eaaw0279 (2019).
  - [19] S. Mahmoodian, G. Calajó, D. E. Chang, K. Hammerer, A. S. Sørensen, *arXiv*: 1910.05828 (2019).
  - [20] H. J. Kimble, *Nature* **453**, 1023 (2008).
  - [21] S. Datta, *Surface Acoustic Wave Devices*, (Prentice-Hall, Englewood Cliffs, NJ, 1986).
  - [22] D. Morgan, *Surface Acoustic Wave Filters*, 2nd ed. (Academic, Amsterdam, 2007).
  - [23] M. V. Gustafsson, T. Aref, A. F. Kockum, M. K. Ekström, G. Johansson, and P. Delsing, *Science* **346**, 207 (2014).
  - [24] R. Manenti, A. F. Kockum, A. Patterson, T. Behrle, J.

- Rahamim, G. Tancredi, F. Nori, and P. J. Leek, Nat. Comm. **8**, 975 (2017).
- [25] T. Petroskya and S. Subbiaha, Physical E **19**, 230 (2003).
- [26] A. Frisk Kockum, P. Delsing, and G. Johansson, Phys. Rev. A **90**, 013837 (2014).
- [27] L. Guo, A. Grimsom, A. F. Kockum, M. Pletyukhov, and G. Johansson, Phys. Rev. A **95**, 053821 (2017).
- [28] A. F. Kockum, G. Johansson, and F. Nori, Phys. Rev. Lett. **120**, 140404 (2018).
- [29] P. Türschmann, H. L. Jeannic, S. F. Simonsen, H. R. Haakha, S. Götzinger, V. Sandoghdar, P. Lodahl, and N. Rotenberg, Nanophotonics **8**, 1641 (2019).
- [30] G. Andersson, B. Suri, L. Guo, T. Aref, and P. Delsing, Nat. Phys. **15**, 1123 (2019).
- [31] A. G.-Tudela, C. S. Muñoz, and J. I. Cirac, Phys. Rev. Lett. **122**, 203603 (2019).
- [32] L. Guo, A. F. Kockum, F. Marquardt, and G. Johansson, arXiv: 1911.013028 (2019).
- [33] S. Guo, Y. Wang, T. Purdy, and J. Taylor, arXiv: 1912.09980 (2019).
- [34] B. Kannan, *et al.*, arXiv: 1912.12233 (2019).
- [35] U. Fano, Phys. Rev. **124**, 1866 (1961).
- [36] J. Koch, T. M. Yu, J. Gambetta, A. A. Houck, D. I. Schuster, J. Majer, A. Blais, M. H. Devoret, S. M. Girvin, and R. J. Schoelkopf, Phys. Rev. A **76**, 042319 (2007).
- [37] W. Zhu, Z. H. Wang, and D. L. Zhou, Phys. Rev. A **90**, 043828 (2014).
- [38] Y. Chu, P. Kharel, W. H. Renninger, L. D. Burkhardt, L. Frunzio, P. T. Rakich, and R. J. Schoelkopf, Science **358**, 199 (2017).
- [39] B. A. Moores, L. R. Sletten, J. J. Viennot, and K. W. Lehnert, Phys. Rev. Lett. **120**, 227701 (2018).